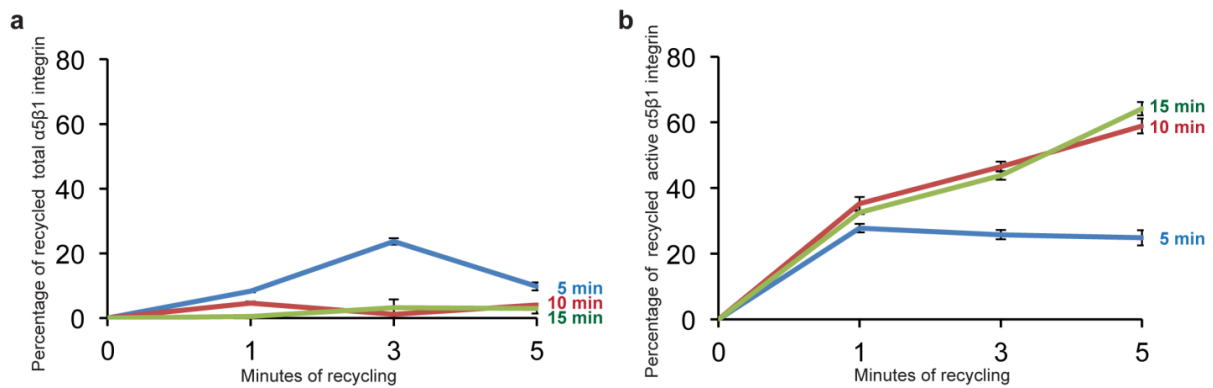
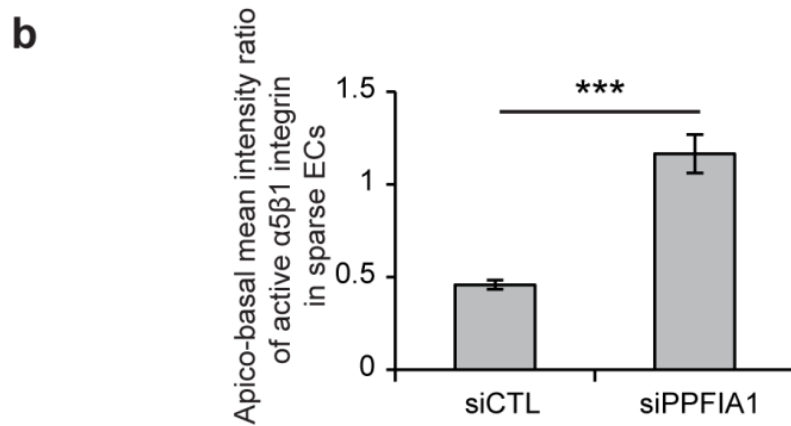
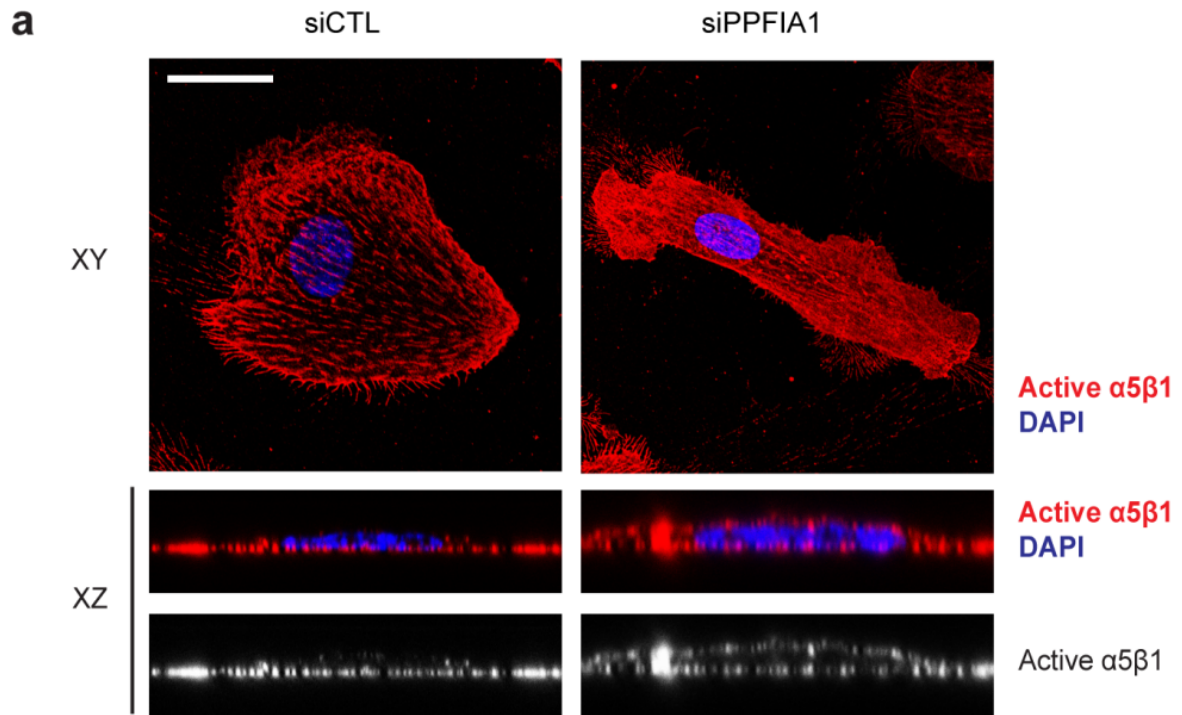


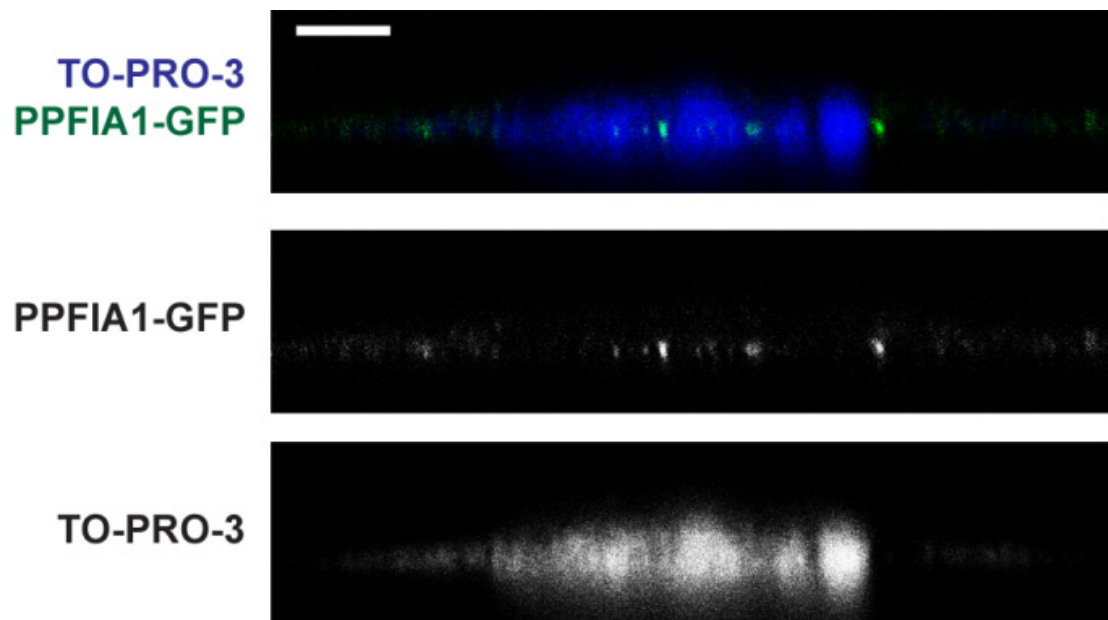
Supplementary Figure 1. 3D reconstruction, distribution, and amount quantification of active and total $\alpha 5$ integrin in ECs. Confocal xy sectioning microscopy analysis and 3D reconstruction of anti-active $\alpha 5$ integrin cell surface localization following 20 minutes of incubation with SNAKA51 mAb (green) and VC5 mAb (red) on living ECs. Side, top, and bottom views as well as quantitative analysis of apico-basal mean fluorescence intensity ratio revealed that while SNAKA51⁺ active $\alpha 5$ integrin localizes on the basolateral surface of ECs, VC5⁺ total $\alpha 5$ integrin is randomly distributed all around the cell surface. Quantitative analysis of apico-basal mean fluorescence intensity ratio of total $\alpha 5\beta 1$ integrin, as recognized by rabbit polyclonal Ab1928 antibody, was performed as further control of VC5 staining. ***P < 0.001, Student's t-test.



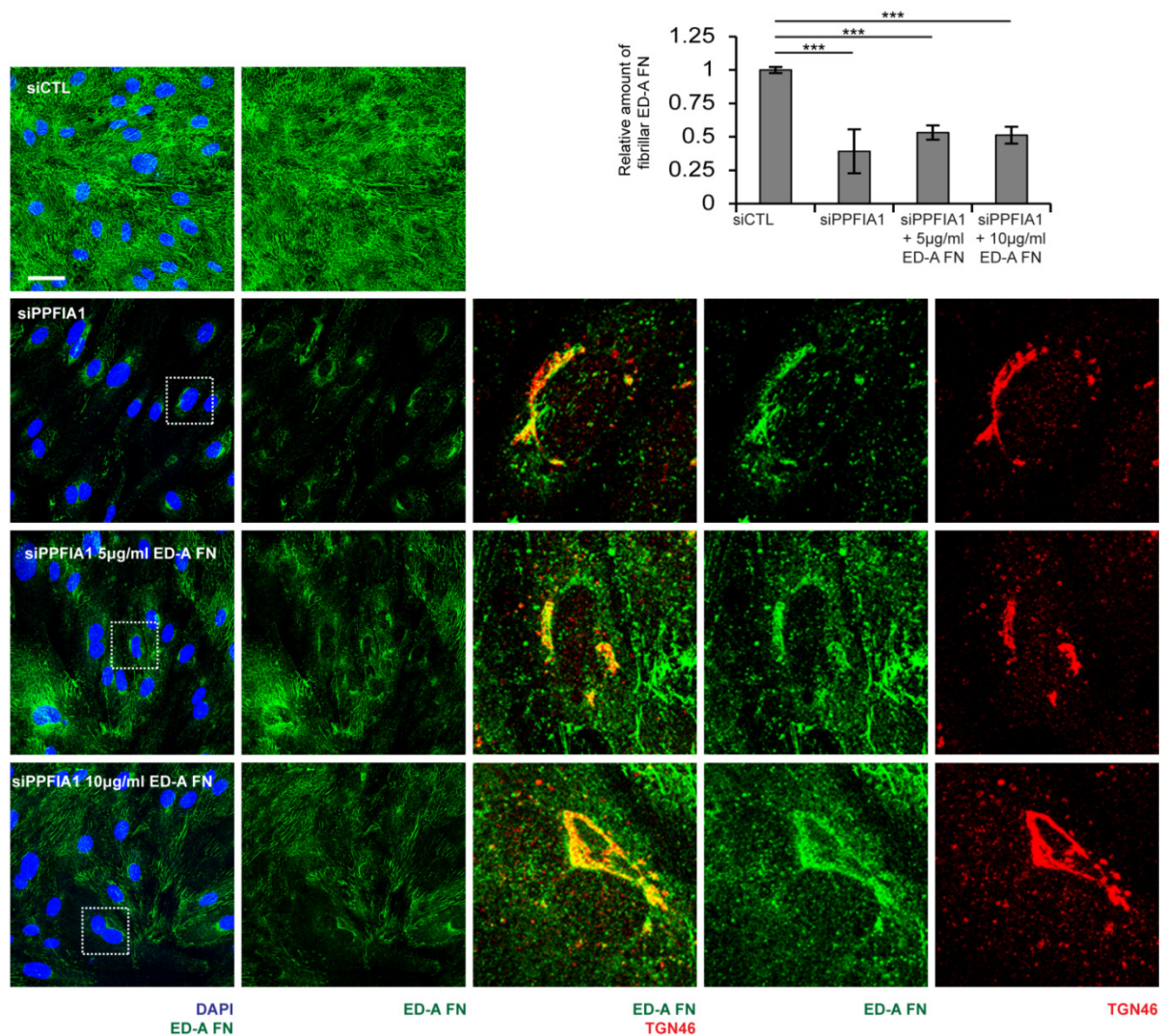
Supplementary Figure 2. In ECs total/inactive, but not active $\alpha 5 \beta 1$ integrin recycles mainly from early endosomal compartments. Time-course analysis of the relative amounts of total/inactive (**a**) or active (**b**) $\alpha 5 \beta 1$ integrins, as respectively recognized by VC5 and SNAKA51 mAbs, which recycle after being left to be endocytosed for different time points. Total/inactive (**a**), but not active (**b**) $\alpha 5 \beta 1$ integrins are only and rapidly recycled to the EC surface within 5 minutes after endocytosis. On the contrary, active (**b**) $\alpha 5 \beta 1$ integrins are recycled to the cell surface also at later time points (10 and 15 min). Values are mean \pm s.e.m., $n = 3$ technical replicates. One out of three independent experiments is shown.



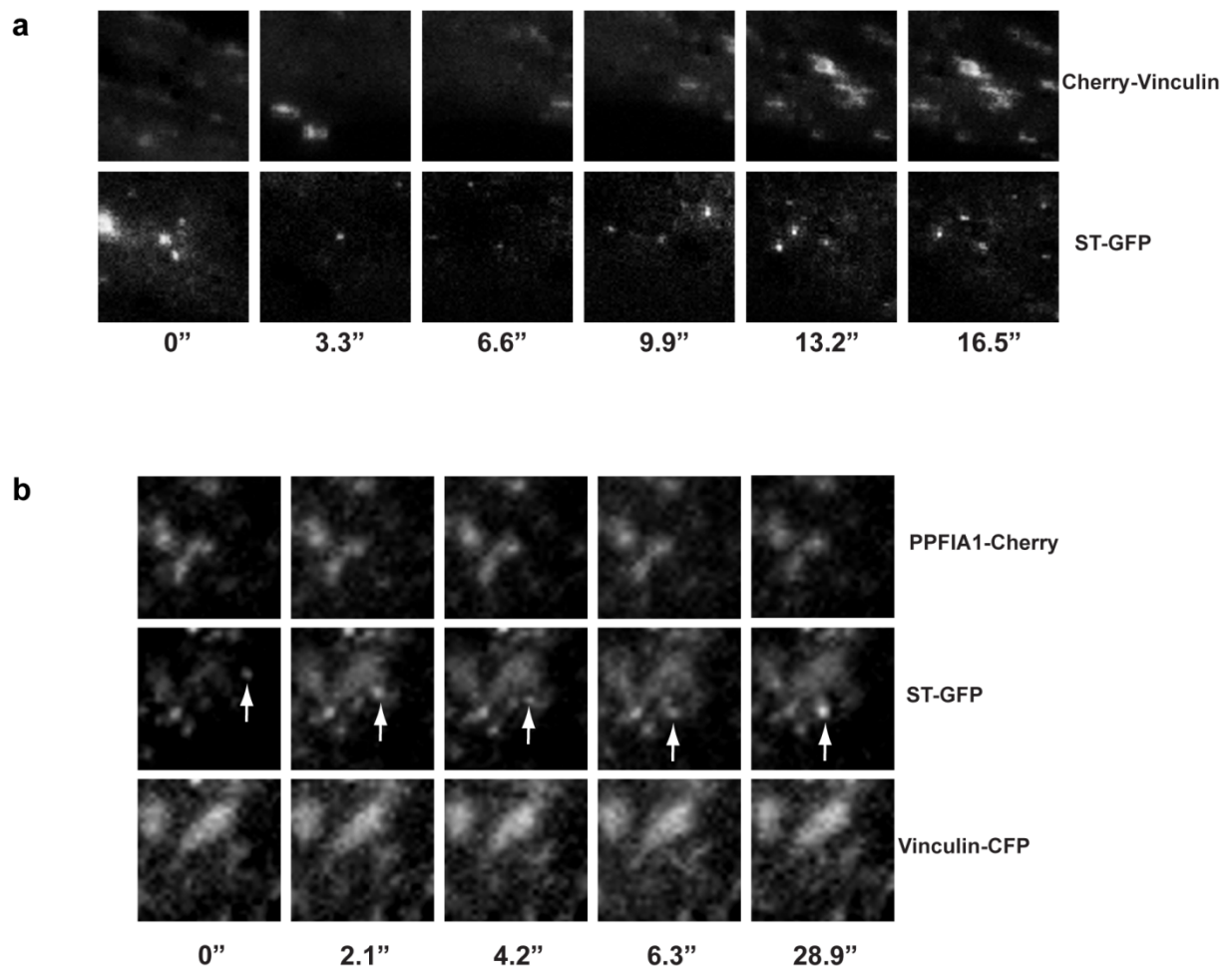
Supplementary Figure 3. PPFIA1 drives basolateral localization of active $\alpha 5\beta 1$ integrin in sparse cells. (a) Confocal xy and xz sectioning microscopy analysis of anti-active $\alpha 5\beta 1$ integrin cell surface localization (red) following 20 minutes of incubation with SNAKA51 mAb on living sparse ECs. (b) Quantitative analysis of apico-basal mean intensity ratio of SNAKA51⁺ active $\alpha 5\beta 1$ integrin. SNAKA51⁺ active $\alpha 5\beta 1$ integrin localizes on the basolateral surface of sparse siCTL, but not siPPFIA1 ECs, in which it randomly redistributes all around the cell surface. Data are mean \pm s.e.m., n = 20 cells per condition pooled from 2 independent experiments. Scale bar, 20 μ m (a) ***P < 0.001, Student's t-test.



Supplementary Figure 4. PPFIA1 localizes on the basolateral surface of ECs. Confocal xz sectioning microscopy analysis of PPFIA1-GFP localization (green) in confluent ECs that were co-stained with the nuclear marker TO-PRO-3. Scale bar, 5 μ m

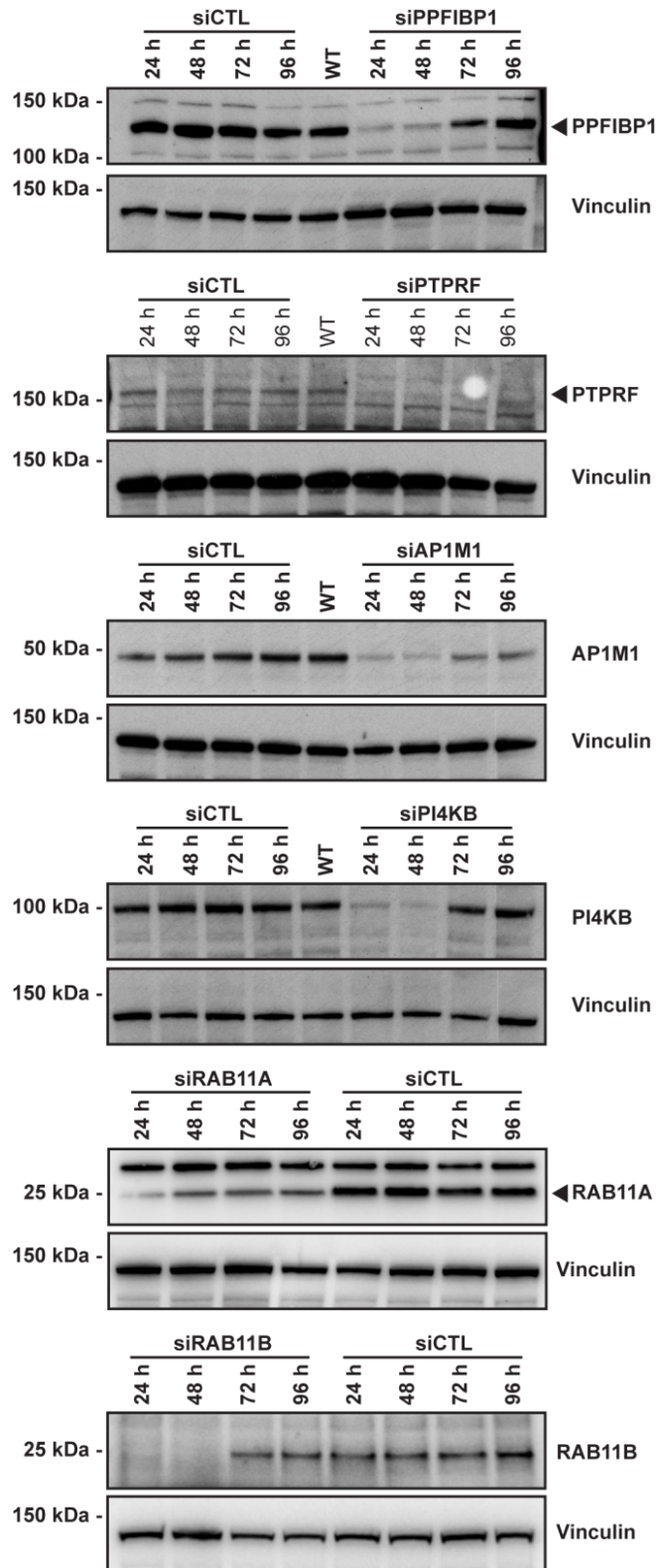


Supplementary Figure 5. Exogenous ED-A FN doesn't rescue basolateral fibrillar FN network in siPPFIA1 ECs. Confocal microscopy analysis of IST-9 mAb-labeled ED-A FN (green) in confluent ECs. ED-A FN polymerizes into a fibrillar network in siCTL, but not in siPPFIA1 ECs in which it accumulates in the TGN46+ (red) TGN cisternae. Exogenously added ED-A FN (5 µg/ml or 10 µg/ml) does not restore basolateral ED-A FN polymerization in siPPFIA1 ECs. The relative amount of fibrillar ED-A FN area was calculated in siCTL, siPPFIA1 and siPPFIA1 + 5 or 10 µg/ml exogenous ED-A FN ECs. Data are mean ± s.e.m., n = 20 cells per condition pooled from 2 independent experiments. Scale bar, 50 µm. ***P < 0.001, Student's t-test.

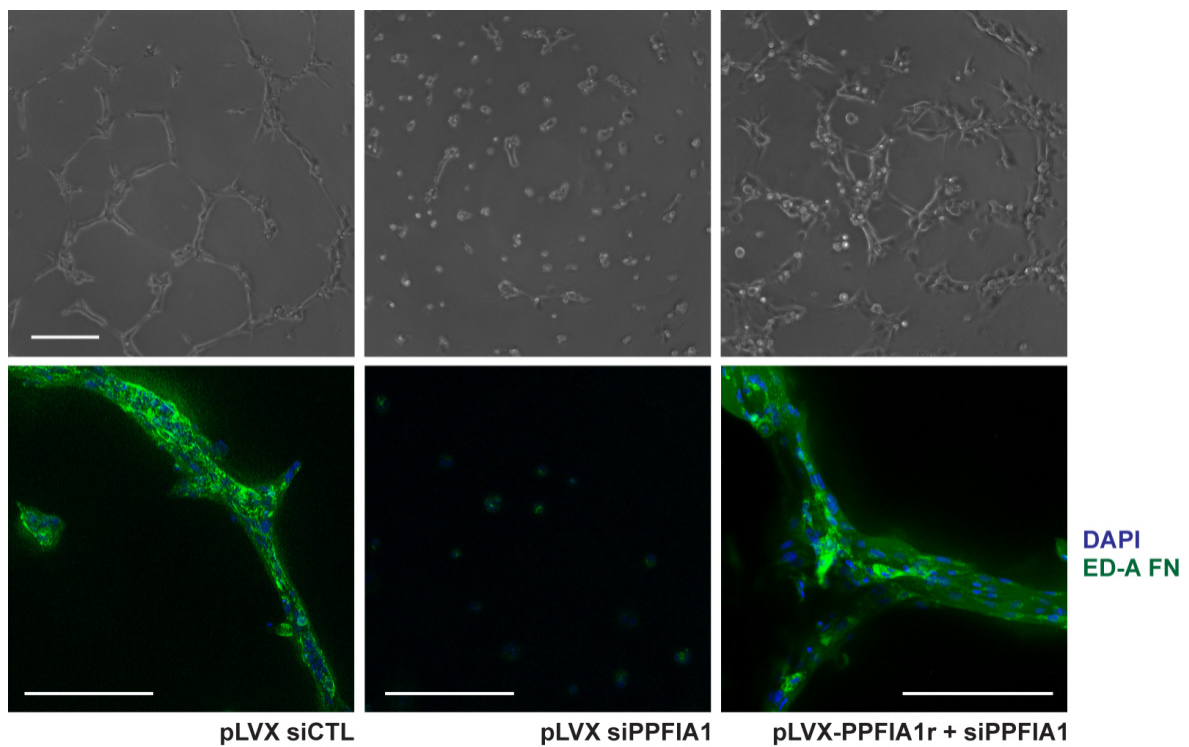


Supplementary Figure 6. Post-Golgi carrier vesicles target endothelial ECM adhesions.

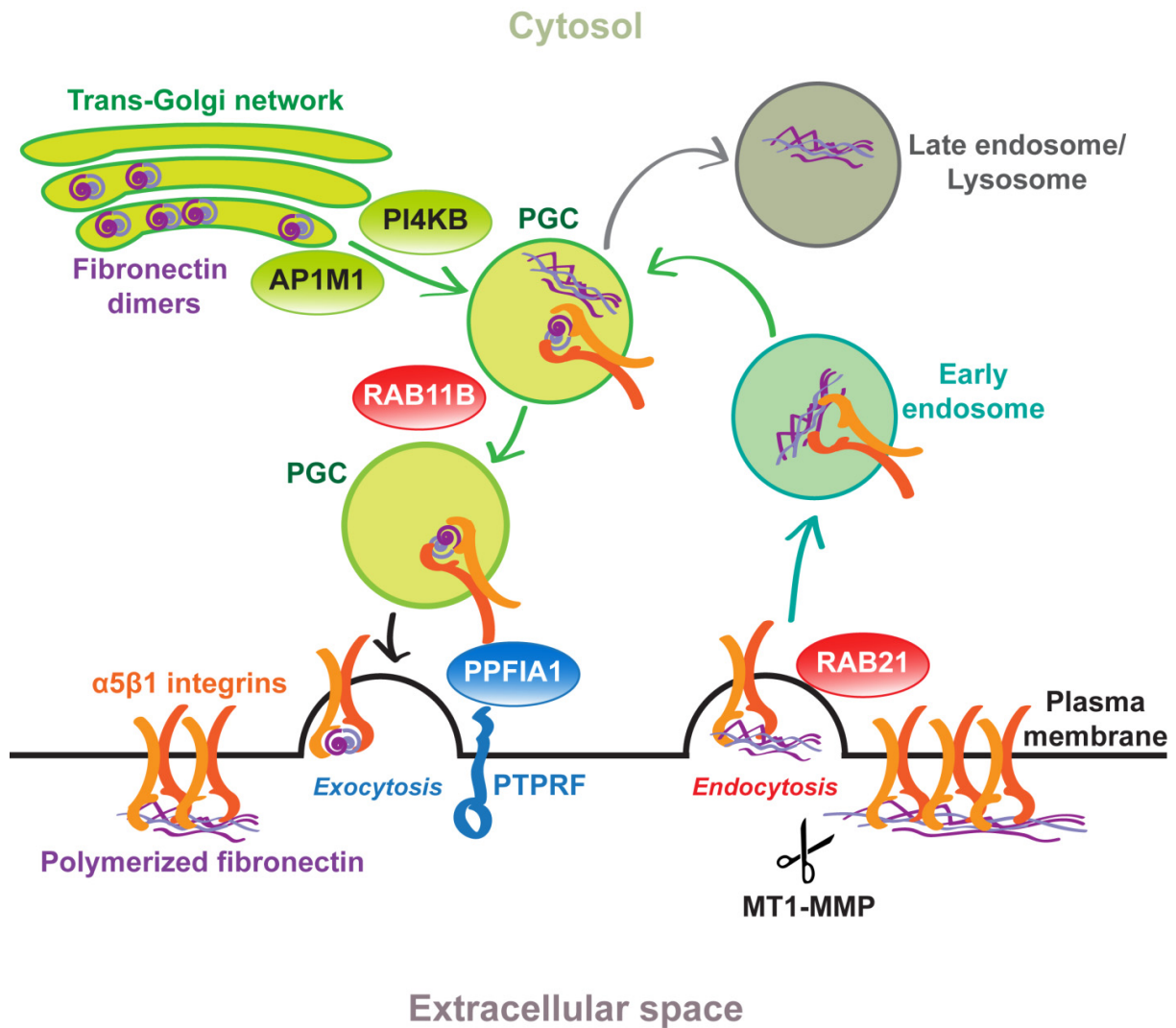
(a, b) Single channel photographs of the magnifications of the snapshots from live time-lapse total internal reflection fluorescence (TIRF) microscopy shown in Figure 5.



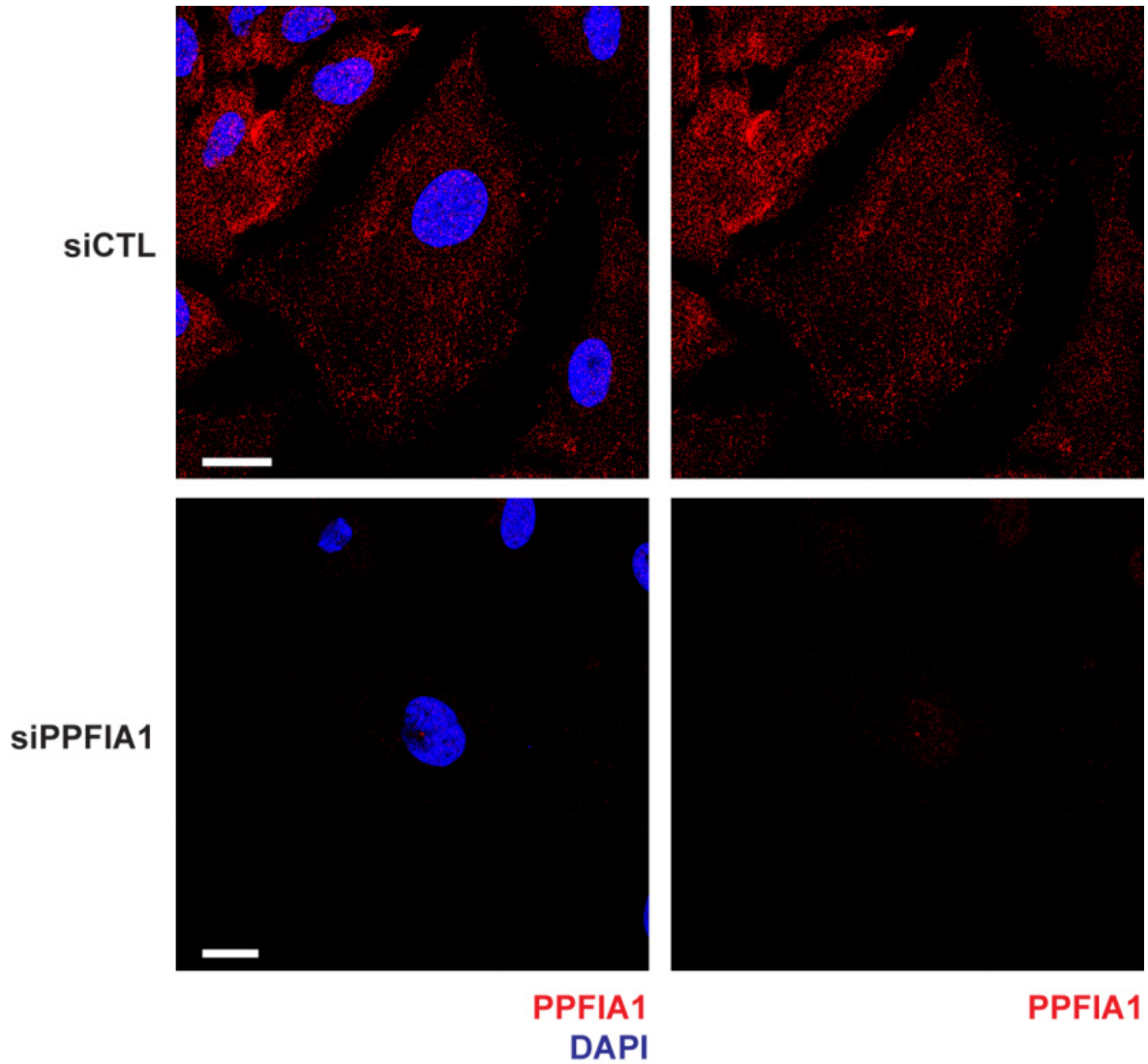
Supplementary Figure 7. Effective siRNA-mediated gene silencing of PPFIBP1, PTPRF, AP1M, PI4KB, RAB11A, and RAB11B proteins in ECs. Western blot analysis of lysates of ECs, control (siCTL), or PPFIBP1 (siPPFIBP1), or PTPRF (siPTPRF), or AP1M1 (siAP1M1), or PI4KB (siPI4KB), or RAB11A (siRAB11A), or RAB11B (siRAB11B) silenced. ECs were lysed 24, 48, 72 and 96 hours after the second siRNA oligofection and proteins were separated by SDS-PAGE and probed for the corresponding Abs. Where more bands are present in Western Blots the arrowhead indicates the one corresponding to the specific protein.



Supplementary Figure 8. PPFIA1 silencing affects vascular morphogenesis in cultured ECs. Representative pictures of vascular networks formed by pLVX siCTL, pLVX siPPFIA1, and pLVX- PPFIA1r + siPPFIA1 ECs plated on growth factor-reduced Matrigel matrix. PLVX siCTL but not pLVX siPPFIA1 ECs form capillary networks that are covered by a dense meshwork of polymerized cellular ED-A fibronectin. PLVX-mediated PPFIA1r overexpression restores capillary network formation and ED-A FN polymerization by siPPFIA1 ECs. Scale bar, 100 μ m.



Supplementary Figure 9. A TGN-hinged signaling pathway couples active $\alpha 5\beta 1$ integrin traffic and fibronectin fibril turnover. In ECs, upon MT1-MMP-dependent cleavage of FN fibrils, FN fragment-bound active $\alpha 5\beta 1$ integrins undergo Rab21 GTPase-driven internalization within early endosomes. From this subcellular location, FN fragment-bound active $\alpha 5\beta 1$ integrins traffic to post-Golgi vesicles (PGCs) that bud, in a PI4KB and AP-1A-dependent manner, from the Trans-Golgi network (TGN) cisternae and contain freshly synthesized FN. Within PGCs, active $\alpha 5\beta 1$ integrins may swap old FN fragments for new FN dimers and the former are likely directed towards the late endosomal/lysosomal compartments for degradation. PGCs containing fresh FN-bound active $\alpha 5\beta 1$ integrins are then directed, on a RAB11B-dependent pathway, towards the basolateral side of ECs. Here, the PTPRF/PPFIA1 complex localizes in close proximity of fibrillar adhesions. Similarly to the function that it plays in neuron presynaptic sites and thanks to its ability to bind the $\beta 1$ cytotail of active $\alpha 5\beta 1$ integrin, PPFIA1 may favor the docking of PGCs containing fresh FN-bound active $\alpha 5\beta 1$ integrins. The ensuing fusion of PGCs with the plasma membrane may favor the targeted local appearance of fresh FN-bound active $\alpha 5\beta 1$ integrins, thus allowing the replacement of old for new FN within fibrils. Finally, a corollary hypothesis may be that, upon endocytosis, active $\alpha 5\beta 1$ integrin-bound non-polymerized FN dimers recycle back to the basolateral EC surface and that this endo-exocytic cycle continues until FN dimers incorporate into fibrils due to polymerization (not depicted).



Supplementary Figure 10. Characterization of rabbit polyclonal anti-PPFIA1 antibody. siCTL or siPPFIA1 ECs were fixed and stained with rabbit polyclonal antibody anti-PPFIA1 and DAPI. Confocal fluorescence microscopy analysis demonstrate that specific PPFIA1 staining present in siCTL ECs is totally absent in siPPFIA1 ECs. Scale bar, 20 μ m.

Figure 1, panel d

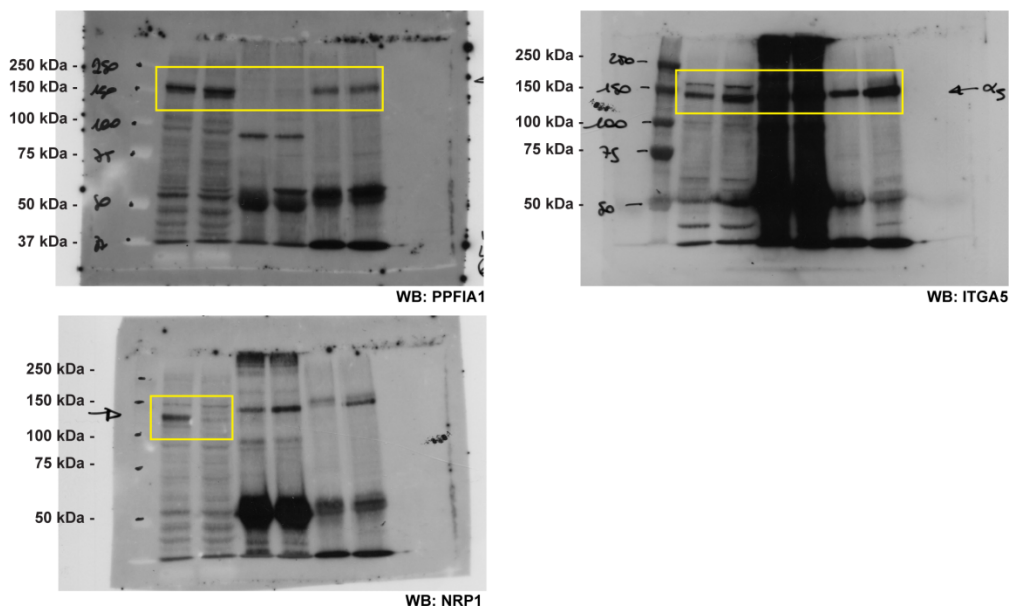
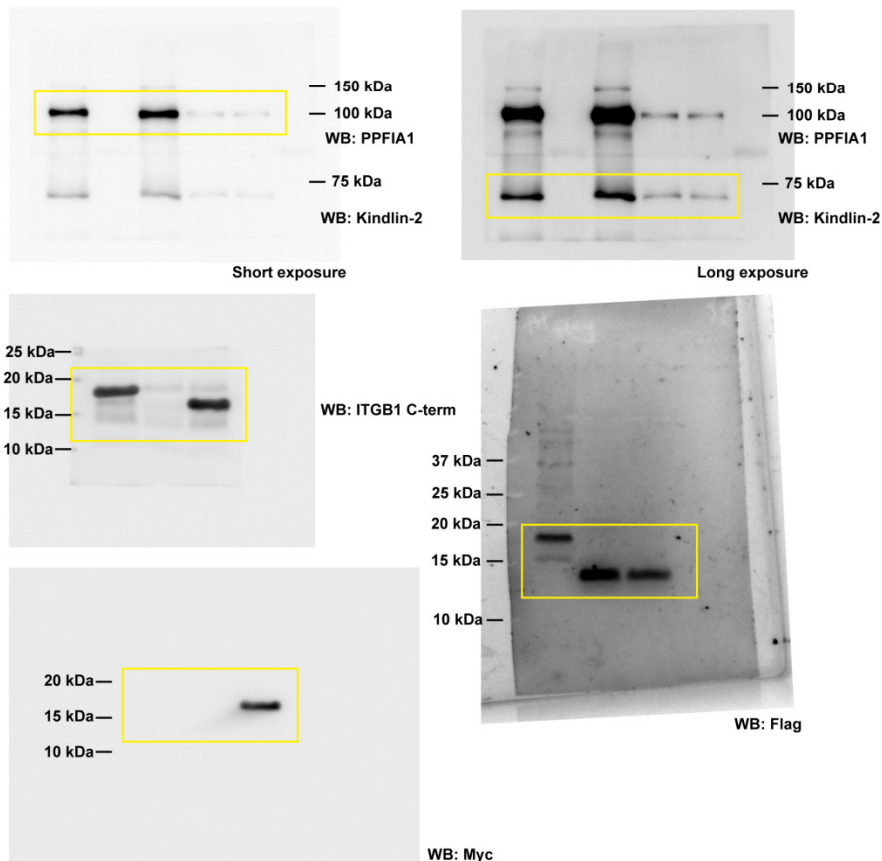


Figure 1, panel e



Supplementary Figure 11. Full images of blots that were cropped in main Figure 1. Yellow squares indicate the cropped images.

Figure 2, panel a

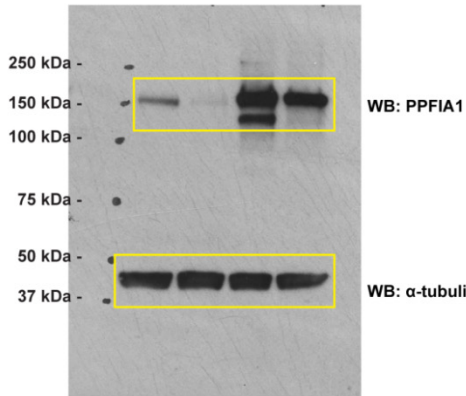


Figure 4, panel e

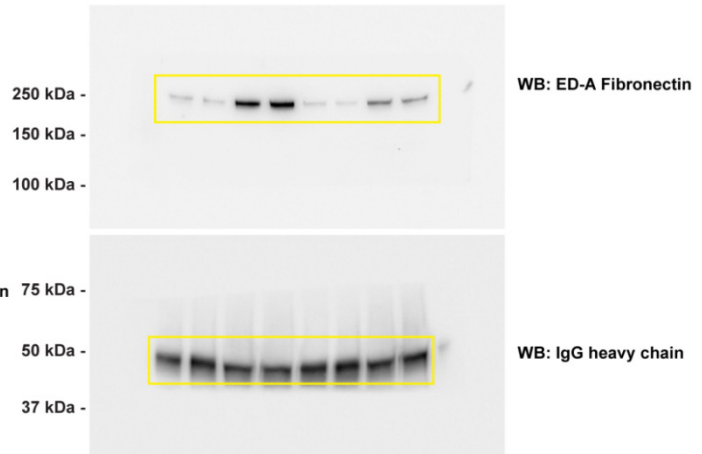
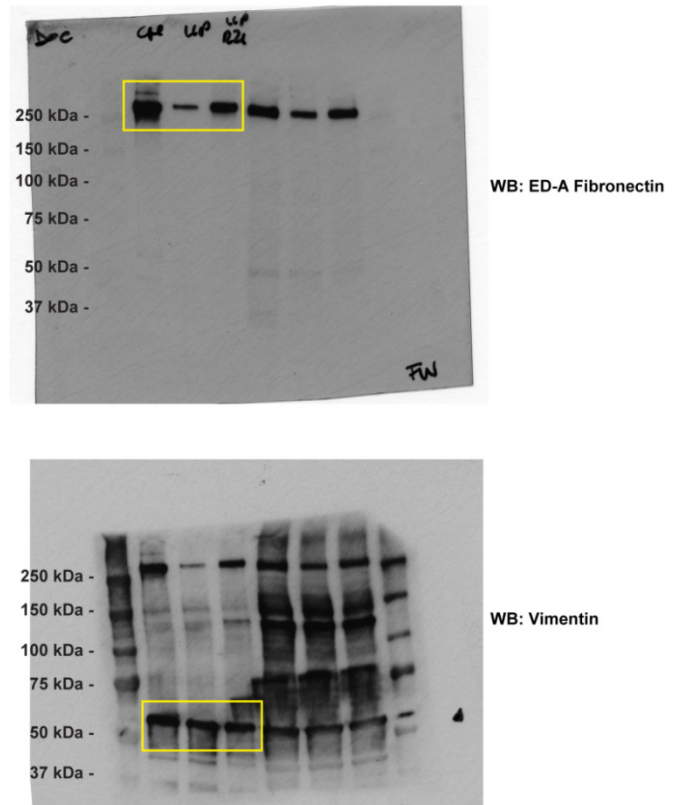
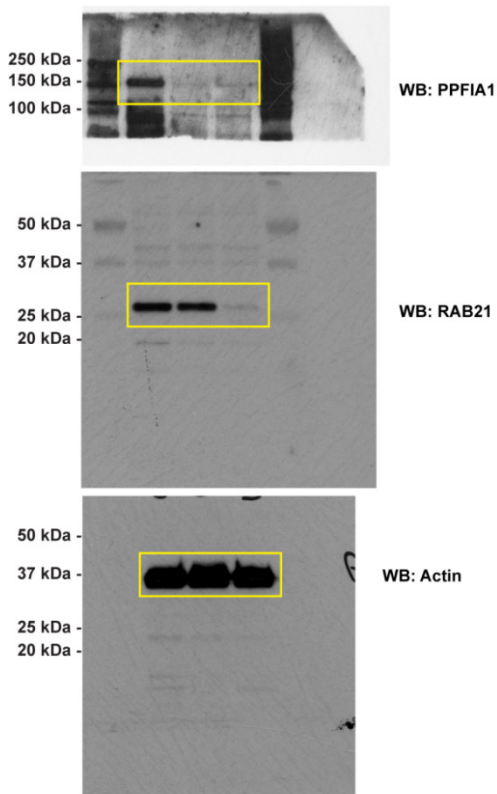


Figure 6, panel b



Supplementary Figure 12. Full images of blots that were cropped in main Figures 2, 4, and 6. Yellow squares indicate the cropped images.

Figure 8, panel e

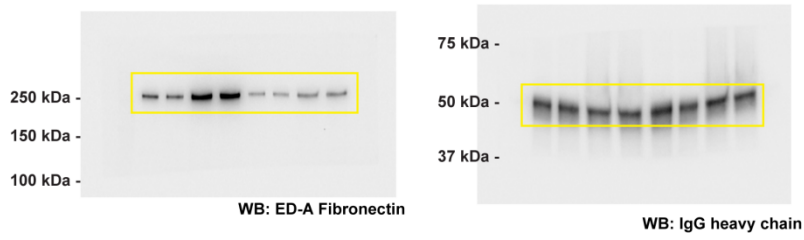


Figure 9, panel a

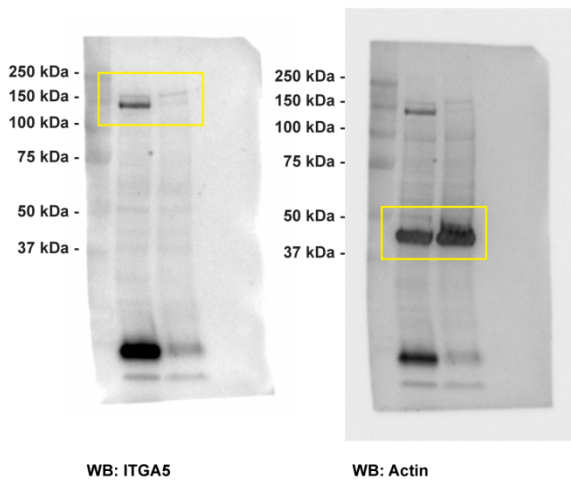


Figure 9, panel c

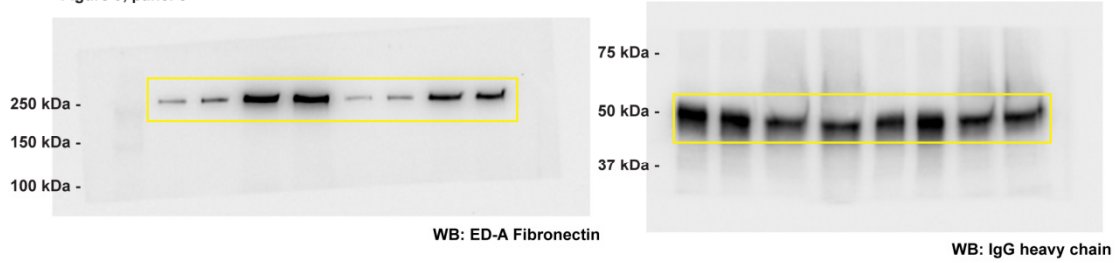
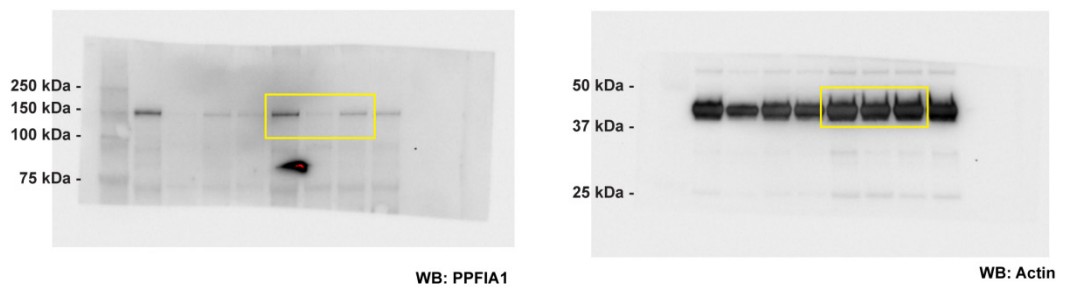
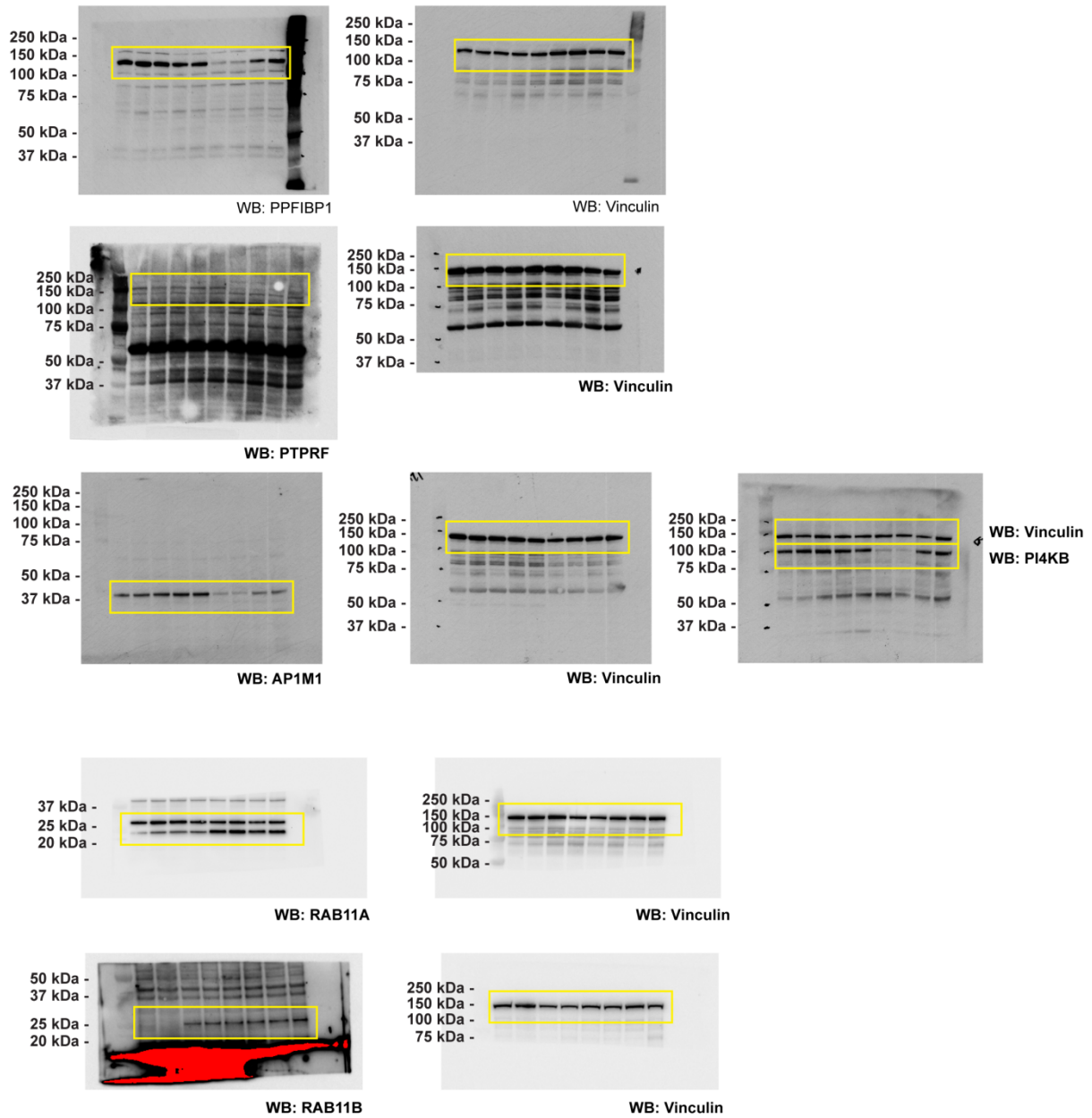


Figure 10, panel b



Supplementary Figure 13. Full images of blots that were cropped in main Figures 8, 9, and 10. Yellow squares indicate the cropped images.

Supplementary figure 7



Supplementary Figure 14. Full images of blots that were cropped in Supplementary Figure 7. Yellow squares indicate the cropped images.

	MO CTL	MO <i>ppfia1</i>	MO <i>ppfia1</i> + mRNA <i>PPFIA1</i>
Injected eggs	226	467	585
Total embryos after 72hpi	154	252	307
Normal embryos	148	166	261
Altered embryos	6	84	47

Supplementary Table 1. Absolute number of MO-CTL, MO-*ppfia1* and MO-*ppfia1*+*PPFIA1* embryos having normal or altered phenotype.

	MO CTL	MO <i>ppfia1</i>	MO <i>ppfia1</i> + mRNA <i>PPFIA1</i>
Normal embryos	96	66	84
Altered embryos	3,8	33,6	15,3

Supplementary Table 2. Relative Percentage of MO-CTL, MO-*ppfia1* and MO-*ppfia1*+*PPFIA1* embryos having normal or altered phenotype.

Antigen	Antibody	Provider	WB	IF	IP
Actin	NB100-74340	Novus Biologicals	1:5000		
AP1M1	12112-1-AP	PTG	1:1000		
EEA1	sc-6415	Santa Cruz		1:200	
Fibronectin	F3648	Sigma		1:200	
Fibronectin	sc-59826 (clone IST9)	Santa Cruz	1:1000	1:100	
Flag	A8592 (clone M2)	Sigma	1:1000		
ITGA5	AB1949	Millipore	1:1000		
ITGA5	SNAKA51	Martin J. Humphries' lab		1:100	1µg/ml
ITGA5	555651 (clone VC5)	BD Biosciences			1µg/ml
ITGB1	AB1952	Millipore	1:2000		
Kindlin-2	Mab2617	Millipore	1:1000		
LAMP1	555798	BD Biosciences		1:50	
Myc	05-419 (clone 9E10)	Millipore	1:1000		
NRP1	sc-7239	Santa Cruz	1:1000		
PI4KB	NBP2-12814	Novus Biologicals	1:1000		
PPFIA1	14175-1-AP	PTG	1:1000	1:50	
PPFIBP1	13961-1-AP	PTG	1:1000		
PTPRF	sc-135969	Santa Cruz	1:500		
Rab11A	TA324158	Origene	1:500		
Rab11B	TA346586	Origene	1:500		
Rab21	Rabbit polyclonal	Johanna Ivaska's lab	1:2000		
TGN46	AHP1586	ABD Serotec		1:100	
TGN46	AHP500	ABD Serotec		1:100	
Vimentin	V5255	Sigma	1:1000		
Vinculin	V9264	Sigma	1:1000	1:400	
α-Tubulin	T5168	Sigma	1:2000		

Supplementary Table 3. Antigen, provider, and dilution used in different experimental settings for all the commercial and non-commercial primary antibodies employed in this study. Western blot (WB), immunofluorescence (IF), and immunoprecipitation (IP).